Journal of Materials Chemistry A

ROYAL SOCIETY OF CHEMISTRY

PAPER

View Article Online
View Journal | View Issue

Check for updates

Cite this: J. Mater. Chem. A, 2025, 13, 17842

Quinone-annulated imidazolium salts as dual electrolyte-sorbents for electrochemical capture of carbon dioxide†

Haley A. Petersen, [ab] Hunter J. Koltunski, [ab] Phuc H. Pham, [ab] Quinn M. Brink, [ab] Ashley Ley, [a] Jonathan Lee, [ab] Oliver M. Wright, [ab] Keenan Wyatt, [a] Richard D. Noble, [a] Abdulaziz W. Alherz *[c] and Oana R. Luca *[ab]

Received 12th February 2025
Accepted 25th April 2025

DOI: 10.1039/d5ta01163a

rsc.li/materials-a

Electro-swing carbon capture is an emerging technology that aims to mitigate increasing concentrations of CO_2 in the atmosphere through the reversible capture and release of CO_2 using applied potentials, rather than heat, as the driving force. Herein, we report the synthesis and characterization of quinone-annulated imidazolium salts that can act as both sorbent and electrolyte in CO_2 capture applications. Through cyclic voltammetry, conductivity measurements, and corroboration by density functional theory (DFT), we report that alkyl substitution of the C2 position of the imidazolium moiety of these salts, along with judicious choice of counterion, is critical for stability of the sorbent. Across several synthetic iterations, we identify a C2-butylated quinone-annulated imidazolium bistriflimide salt that possesses promising CO_2 binding strengths for capture of CO_2 from dilute sources, relatively small potential difference (ΔE) between the voltage needed for capture and release, a relatively high solubility (2.87 M) in anhydrous acetonitrile, and sufficient solution conductivity to operate as its own electrolyte. This work sets the stage for the design of ionic molecular materials that can act as both reactive sorbents and electrolytes that could ultimately allow for organic redox battery-like operation of electro-swing systems.

Introduction

Electricity-based alternatives to thermal and pressure swing carbon capture technologies are an active area of research due to their potential coupling to renewables.[1–6] In electro-swing carbon capture, a sorbent is activated at an electrode surface under one applied potential and then regenerated under a different potential, rather than requiring a change in temperature or pressure. As shown in Fig. 1, the sorbent is typically activated under negative, cathodic potentials which reduce the sorbent to a strongly nucleophilic state that binds CO_2. The sorbent can then be pumped to the opposite electrode, or alternatively, the electrode originally used to activate the sorbent can be switched to a more positive potential. Under these conditions, the sorbent is oxidized back to the inactive state and CO_2 is released. The regenerated sorbent can then be reused to capture more CO_2.

Within the realm of electro-swing carbon capture, quinone-based sorbents have attracted attention in recent years.[4] Early work by Noble and coworkers[7] on 2,6-di-*tert*-butyl-1,4-benzoquinone set the stage for quinone-based carbon capture by demonstrating that quinoid molecular sorbents can be used to harvest CO_2 from dilute streams of <1% CO_2 in nitrogen and to release back at 1 atm. More recently, Hatton and coworkers demonstrated faradaic electro-swing in a carbon capture device in which quinones tethered to the electrode are able to reversibly capture CO_2 when reduced and release it when oxidized (Fig. 2).[1]

These studies sparked increasing interest in the study of quinones for electrochemical carbon capture.[8–10] Despite the

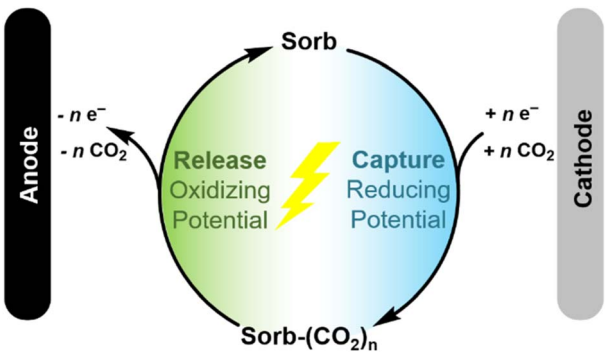

Fig. 1 Schematic of an electro-swing carbon capture system.

[a]Department of Chemistry, University of Colorado Boulder, Boulder, Colorado 80309, USA. E-mail: oana.luca@colorado.edu

[b]Renewable and Sustainable Energy Institute and Materials Science and Engineering Program, University of Colorado Boulder, Boulder, Colorado 80309, USA

[c]Department of Chemical Engineering, College of Engineering and Petroleum, Kuwait University, Safat 13060, Kuwait. E-mail: abdulaziz.alherz@ku.edu.kw

† Electronic supplementary information (ESI) available. CCDC 2417570. For ESI and crystallographic data in CIF or other electronic format see DOI: https://doi.org/10.1039/d5ta01163a

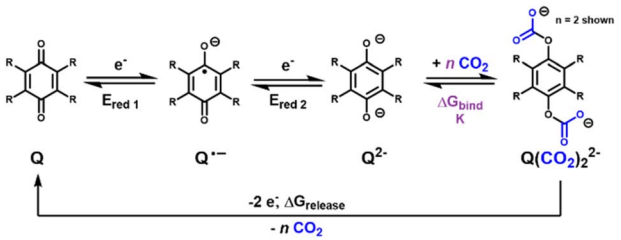

Fig. 2 CO_2 binding mechanism for a generic tetrasubstituted 1,4-quinone.

promising nature of these systems, many studies identified challenges in the form of insufficient selectivity, efficiency, and stability in the presence of oxygen, compared to benchmarks for industrial relevance. Excitingly, Hatton and coworkers have recently reported that a particular benzodithiophene annulated quinone can serve well as an oxygen impervious quinone for direct air capture (DAC).[11] To further address these challenges, we sought to design improved electro-swing ionic liquid-like molecular sorbents that can (a) reversibly bind CO_2 in an electro-activated fashion with a minimal difference between capture and release potentials, (b) show a sufficiently negative ΔG_{bind} in reduced forms for operation in dilute CO_2 streams,[12] and (c) can operate without the need for supporting electrolyte.

We hypothesized that the structure would leverage a combination of synthetic versatility and access to reversible, electro-activated CO_2 capture of the quinone family to target goal (a). Additionally, our prior work suggests that with appropriate selection of electron-donating or -withdrawing functionalities, quinones also reach binding strengths sufficient to achieve goal (b).[13] Finally, we hypothesized that adding an imidazolium functionality would serve as a redox-stable positive charge tag that could remain intact under the desired operating potentials, enabling the synthesis of a sorbent salt that can, in principle, render the solution conductive without the need for supporting electrolyte (c). This positive charge tag also shifts the reduction potential of the parent molecule to more positive potentials, increasing the likelihood of achieving sorbent activation at potentials positive of oxygen reduction. Additionally, imidazolium-based room-temperature ionic liquids (RTILs) are known to possess limited oxygen solubility and enhanced CO_2 solubility, thereby increasing the local concentration of CO_2 substrate and limiting the potentially deleterious presence of oxygen.

In addition, quantum chemical density functional theory (DFT) was implemented to calculate optimized geometries and energies of all starting quinone-based materials, their first and second electrochemically reduced forms, and their corresponding CO_2 bound structures.[14] Through these assessments, experimental data revolving around newly synthesized quinone sorbents were corroborated.

Results & discussion

Based upon the general principles outlined above, we identified the molecule candidates **1–6** (Fig. 3), which had not been previously studied for carbon capture applications.[15–17]

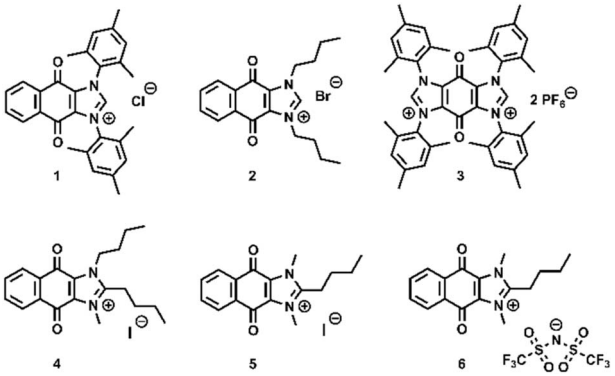

Fig. 3 Structures of the imidazolium-annulated quinone carbon capture sorbents.

Compounds **1** and **3** were synthesized according to literature procedure.[15,18,19] Compound **2** was synthesized following a modification of a literature procedure for the synthesis of the analogous bromide salt[20] by substituting 1-iodobutane for 1-bromobutane in the final synthetic step, thus yielding the bromide salt as the final product. Synthetic details and characterization of compounds are available in our ESI Section S3.† The N-substitutions of compounds **4–6** were also carefully selected with the aim of disrupting solid packing and increase the likelihood of obtaining an ionic liquid to mitigate oxygen solubility. We hypothesized that these changes would preserve CO_2 binding reactivity while encouraging ionic liquid-like behavior. The structures of sorbents **5** and **6** are more easily synthesized due to symmetrical methylation, while sorbent **4** maximizes solid packing disruption and organic solubility using an *N*-butyl group.

Cyclic voltammetry studies

CV experiments were undertaken to assess the CO_2 binding characteristics of the sorbent candidates. Unless otherwise noted, CVs were collected with 0.1 M NBu_4PF_6 supporting

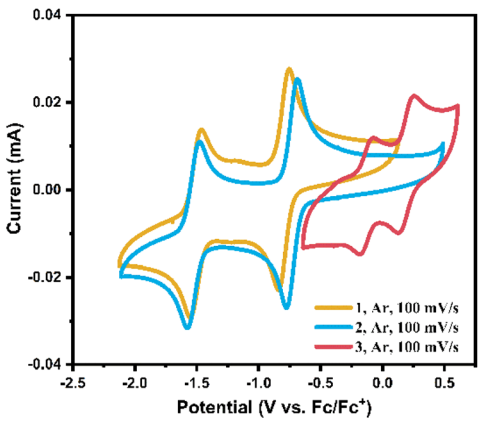

Fig. 4 CVs of 1 mM solutions of compounds **1** (yellow), **2** (blue), **3** (red) under Ar in 0.1 M NBu_4PF_6 in MeCN collected with a scan rate of 100 mV s^{-1} – glassy carbon working electrode, Pt wire counter electrode, reference externally *vs.* Fc/Fc^+.

Table 1 Summarizing and comparing DFT values and experimental values for all sorbents

Compound	Experimental E_{red2} (V *vs.* Fc/Fc$^+$)	Experimental E_p, capture (V *vs.* Fc/Fc$^+$)	$\Delta E_{release-capture}$ (V)	DFT E_{red2} (V *vs.* Fc/Fc$^+$)	DFT E_p, capture (V *vs.* Fc/Fc$^+$)	Experimental ΔG_{bind} (kcal mol^{-1})	DFT ΔG_{bind} (kcal mol^{-1})	Difference ΔG_{bind} (kcal mol^{-1})	Experimental CO_2 binding stoichiometry
1	−1.5	−1.38	0.32	−2.05	−1.47	−5.3	−4.9	0.4	1
2	−1.53	−1.34	0.53	−2.09	−1.53	−5.2	−3.9	1.3	1
3[a]	−0.13	n/a	n/a	n/a	n/a	n/a	n/a	n/a	n/a
4	−1.55	−1.38	0.26	−2.02	−1.44	−5.9	−7.9	2	1
5	−1.51	−1.31	0.61	−2.08	−1.53	−5.7	−6.7	1	1
6	−1.55	−1.39	0.67	−2.08[b]	−1.53[b]	−5.6	−6.7[b]	0.9	1

[a] No binding observed for this compound. [b] Binding is attributed to the quinone species and not the counter ion, hence, these values were not calculated as they would be identical to compound **5**.

electrolyte in anhydrous MeCN with a 3 mm glassy carbon working electrode, Pt wire counter electrode, and single-junction silver wire pseudoreference electrode referenced externally to the ferrocene/ferrocenium redox couple. CVs of 1 mM solutions of compounds **1–3** in 0.1 M NBu_4PF_6 in anhydrous MeCN are presented in Fig. 4.

These CVs reveal the expected two reversible reduction features for each of the compounds, attributed to the two one-electron quinone-centered reductions standard for quinones in aprotic solutions. Comparison of the three compounds reveals that substitution of the *N*-mesityl groups of **1** for *N*-butyl groups in **2** does little to impact the observed reduction potentials. This observation is also consistent with the quinone-centered nature of the two reductions under study, which are not anticipated to be strongly electronically influenced by the identity of the imidazolium wingtips. On the other hand, installation of a second positive charge in structure **3** results in a drastic positive shift in the observed potentials, changing the observed second reduction potential by nearly 1.5 V (Fig. 4).

In further support of our hypothesis that the addition of a positively charged imidazolium group would shift the reduction potentials of naphthoquinone-based compounds **1** and **2** more positive than those of their parent compounds, their second reduction potentials do in fact lie approximately 300 mV positive of those of the parent compound napthoquinone NQ (−1.82 V *vs.* Fc/Fc$^+$).[13] However, the second reduction potentials of **1** and **2** remain just negative of the O_2 reduction potential in dry MeCN.

Based on these observations and the correlation between second reduction potential and CO_2 binding strength of quinones as observed in our previous work, we hypothesized that quinone-annulated imidazolium salts **1** and **2** would have similar values of ΔG_{bind} in their doubly reduced forms, while the corresponding reduced form of compound **3** would have a much less favorable, or perhaps even nonspontaneous, value of ΔG_{bind}.[13]

We proceeded to experimentally determine ΔG_{bind} for each of the three quinones following the experimental protocol outlined in our prior work.[13] Final results for ΔG_{bind} and the best-fit CO_2 binding stoichiometry are reported in Table 1. These analyses are done through titrations of incremental amounts of CO_2 by cyclic voltammetry (Fig. 5a). Specifically, the shift of a second reduction of the quinone is utilized to determine the strength of CO_2 binding of the quinone molecular sorbent. Fig. 5 and S6.3† illustrate relatively strong CO_2 reactivity for both compounds **1** and **2**. Through these analyses, we observed that the two compounds have nearly identical CO_2 binding free energies as expected for two molecules with similar second reduction potentials. The similar reactivity of compounds **1** and **2** is further supported by the nearly identical computed charge densities around the reactive reduced oxygen atom and the bound CO_2, as shown in Fig. S11.4 and S11.8.† In addition, both experimentally determined free energies lie negative of the −4.64 kcal mol^{-1} limit needed for capture from dilute sources such as air.[14]

Lastly, oxidation features that grow in at increasing concentrations of CO_2 are attributed to CO_2 adduct reoxidation and CO_2 release. Under 100% CO_2, **1** is found to have especially promising CO_2 release properties ($\Delta E_{release-capture}$ = 0.32 V). This small potential difference compares favorably even to particularly weakly CO_2 binding quinones with strong electron-withdrawing groups (approx. 400 mv).

Contrary to the reactivity observed for compounds **1** and **2**, compound **3** does not bind CO_2 upon reduction (Fig. S6.4†). No shift in second reduction potential is observed in the presence of CO_2, even when a slow scan rate of 25 mV s^{-1} was employed to allow maximal time for the chemical step of CO_2 binding to take place. The only difference observed between scans of **3** under Ar and under 100% CO_2 is a slight increase in current, which can be attributed to an increase in analyte concentration from evaporative losses while sparging the analyte solution to saturate it with CO_2.

Based on these results, sorbents **1** and **2** were considered for further examination. The two sorbents possess nearly identical reduction potentials and CO_2 binding strengths, and both possess CO_2 binding stoichiometries of 1 equivalent of CO_2 per active sorbent molecule. Despite these similarities, **1** is distinguished by an improved $\Delta E_{release-capture}$ metric and greater synthetic ease. Sorbent **1** was therefore selected for further study.

The compatibility of **1** with electrochemical CO_2 capture conditions was then verified *via* additional CV experiments (Fig. S6.1 and S6.2†). Furthermore, **1** was found to be redox stable in MeCN across a potential window spanning +0.52 to

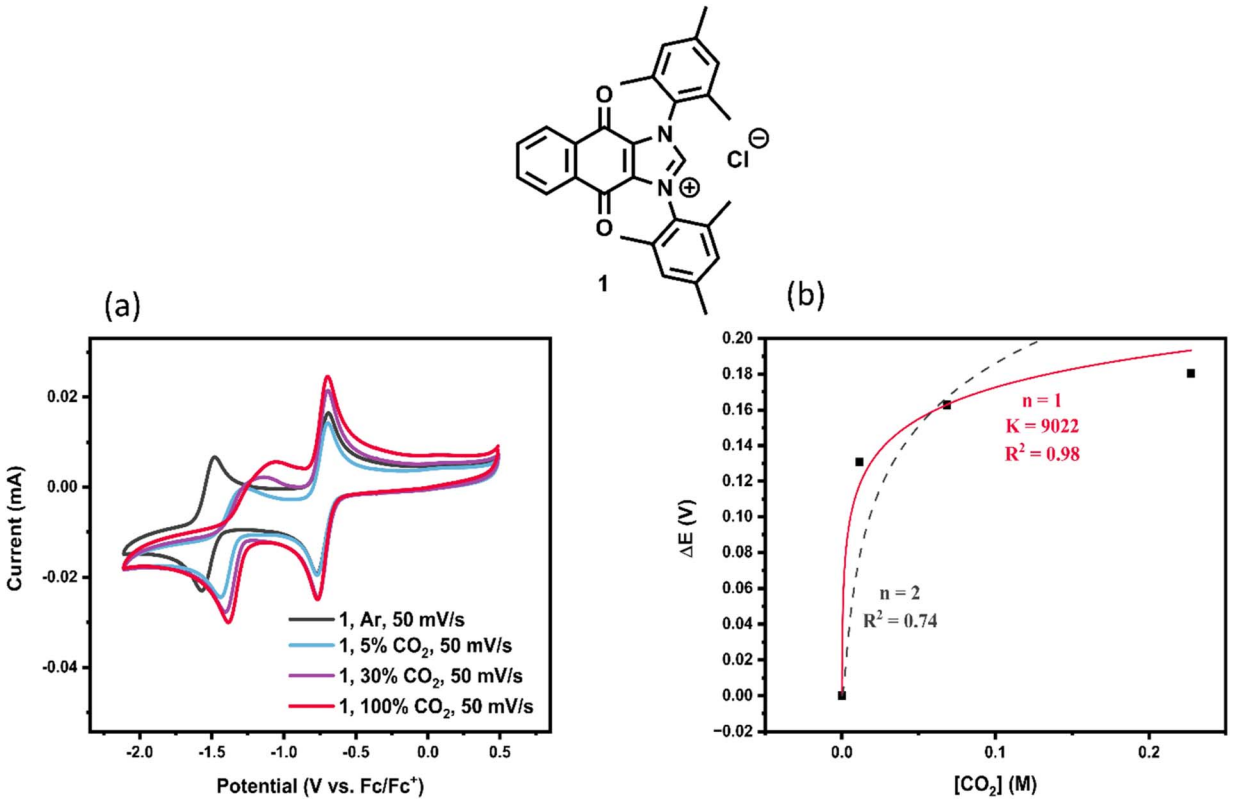

Fig. 5 (a) 1 mM CVs of **1** under varying concentrations of CO_2 (black under argon, cyan under 5% CO_2, purple 30% CO_2, red 100% CO_2) collected with a scan rate of 50 mV s^{-1} in 0.1 M NBu_4PF_6 in MeCN – WE glassy carbon, Pt wire counter electrode, reference externally *vs.* Fc/Fc^+. (b) Plot of ΔE *vs.* $[CO_2]$ fit to $\Delta E = \frac{RT}{F}\ln(K[CO_2]^n + 1)$ to find the equilibrium constant K and stoichiometry n of CO_2 molecules binding to sorbent.

−2.85 V *vs.* Fc/Fc^+, as determined by the onset of undesired irreversible features under inert atmosphere. When this analysis is extended to atmospheres containing CO_2, the sorbent remains stable up to anodic potentials of +0.52 V, while the onset of the irreversible reduction attributed to generation of the free N-heterocyclic carbene (NHC) moves slightly more positive with increasing CO_2 levels, up to −2.3 V *vs.* Fc/Fc^+. As hypothesized, these results suggest that the reduction potential of the imidazolium functionality to its corresponding free NHC lies well outside the operating potential required to generate the doubly reduced active sorbent. This indicates that imidazolium-fused quinones offer a promising method of maintaining redox-impervious charge tags, an important prerequisite for sorbent-electrolytes.

For **1** to act as a sorbent-electrolyte, it must have sufficient solubility in the desired solvent to render the resulting solution conductive without the need for supporting electrolyte. Additionally, the higher the solubility that the compound possesses, the higher the CO_2 capture capacity of **1**-saturated solutions becomes. To assess this metric, we next determined the solubility of **1** in anhydrous MeCN using quantitative ^{1}H-NMR with a known concentration of mesitylene as internal standard (ESI Section S5†). Maximum solubility in anhydrous acetonitrile at room temperature (21 °C) was determined to be 0.12 M, which exceeds the standard 0.1 M supporting electrolyte concentration typically used. CV analysis demonstrates that 0.1 M **1** renders a solution sufficiently conductive to pass current (Fig. 6), with an ionic conductivity of 0.00253 S cm^{-1} (ESI Section S7†).

The CVs presented in Fig. 6 indicate that **1** operates as a combined sorbent-electrolyte by (1) demonstrating solution conductivity in the absence of supporting electrolyte and (2) illustrating CO_2 binding as evidenced by the substantial shift in the second reduction potential under CO_2. Large peak-to-peak separations are observed due to ohmic drop from solution

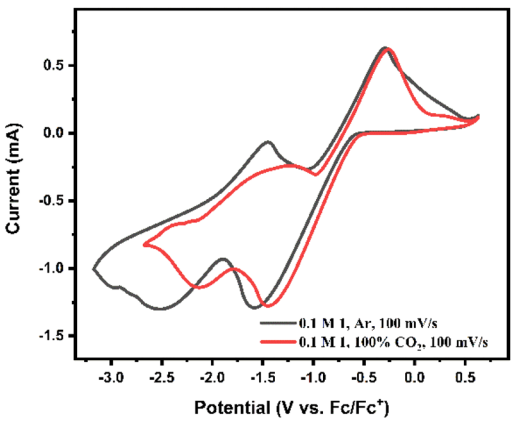

Fig. 6 Supporting electrolyte-free CVs of 0.1 M **1** in MeCN under 100% CO_2 (red) and Ar (black), collected at a scan rate of 100 mV s^{-1} – WE glassy carbon, Pt wire counter electrode, reference externally *vs.* Fc/Fc^+.

resistance, the effects of which become more noticeable when large currents are passed. Notably, however, the CO_2 release feature identified in Fig. 6 does not appear clearly in concentrated conditions, and it is difficult to distinguish between a possible CO_2 release feature and a return oxidation of the doubly reduced sorbent due to the high peak-to-peak separation observed in these conditions.

To assess the water stability of **1**, we evaluated 1 mM solutions of **1** in 95 : 5 MeCN : H_2O by CV (Fig. S6.2†). In the presence of a proton donor, the quinone reduction potentials shift more positive, consistent with literature observations.[3,21] However, the reversibility of the quinone-centered redox features remains intact, suggesting no water-induced degradation of the reduced species over the timescale of the CV. Literature concerning imidazolium-based compounds in other subfields, particularly in the anion exchange membrane community, report sensitivity of imidazolium-based compounds to alkaline conditions, much like that observed for sorbent **1**.[22,23] In some cases, installation of a new alkyl or aryl group at C2 improved stability of compounds for these applications.[24]

Stability studies of 1

Despite promising preliminary results over the course of CV experiments, solutions of **1** employed in these electrochemical analyses were observed to gradually change color from bright yellow to progressively more orange and then red over the course of hours to days. These changes appeared to be more prominent in experiments which employed either ambient atmosphere or water. Notably, the authors of the original synthesis of **1** report that **1** appears to be mildly air sensitive, although this behavior was not observed in the solid state in our hands.[15] To investigate this degradation, after experiments were complete, CV samples were dried *in vacuo* and then extracted with diethyl ether (in which both **1** and supporting electrolyte NBu_4PF_6 are insoluble). A bright red ether-soluble solid was recovered in trace amounts by this method, isolated, and characterized by ^{1}H NMR.[15]

While dissolution of **1** in water and addition of acidic aqueous solution (dilute HCl) had no immediate effect, addition of basic solutions (pH > 10) of NaOH or Na_2CO_3 resulted in the immediate formation of red-purple solids. These solids were filtered from the aqueous solution, dried to a vibrant red solid, and confirmed to exhibit ^{1}H NMR signals consistent with those found in the post-CV samples. Additionally, the same product could be obtained more slowly and in lower yields by preparing a 1 mM solution of **1** in a 50 : 50 mix of MeCN and neutral water and allowing to stir at room temperature overnight.

The degradation product was then crystallized as red plates through slow evaporation from a solution of 1 : 1 MeCN : H_2O, and the resulting crystals were analyzed *via* single-crystal X-ray diffraction (SCXRD) using a Bruker AXS D8 Quest with Cu Kα radiation. The resulting structure, compound **1′**, is presented in Fig. 7.

The resulting structure is consistent with electrospray ionization high-resolution mass spectrometry (ESI-HRMS) data and final ^{1}H NMR assignment for the compound, performed with the assistance of COrrelated SpectroscopY (COSY) NMR (See ESI†).

The product identity confirmed qualitative observations that water, and particularly basic aqueous solutions, promoted degradation of **1**. As shown in Fig. 8, compound **1** degrades by a net addition of OH^- to the imidazolium moiety, opening the imidazolium ring and resulting in the observed neutral red product. Such reactivity is undesirable, as the charge tag in our electrolyte is lost. When this reaction proceeds in the presence of neutral water, sorbent degradation occurs with cogeneration of HCl. When accumulated in sufficient amount, this may further promote unwanted side reactions such as hydrogen evolution under cathodic potentials.

Although **1** was characterized in the solid state, we hypothesized that highly concentrated solutions of **1** in MeCN may demonstrate suppressed oxygen solubility in a fashion similar to their imidazolium-based room temperature ionic liquid (RTIL) counterparts. To investigate this hypothesis, we examined a concentrated solution of **1** under air. When a 0.1 M solution of **1** in MeCN is equilibrated under air at ambient 0.82 atm pressure, the resulting CV shown in Fig. S6.8† exhibits a new feature which we attribute to oxygen reduction. The peak current of this feature (as measured from a linear extrapolation of the baseline) is 51 μA, nearly equivalent to the 58 μA feature observed in standard air-saturated 0.1 M NBu_4PF_6 MeCN solution as seen in Fig. S6.1.† Assuming a similar diffusion coefficient for O_2 in both MeCN solutions (regardless of electrolyte identity), this suggests that O_2 has a similar solubility in each

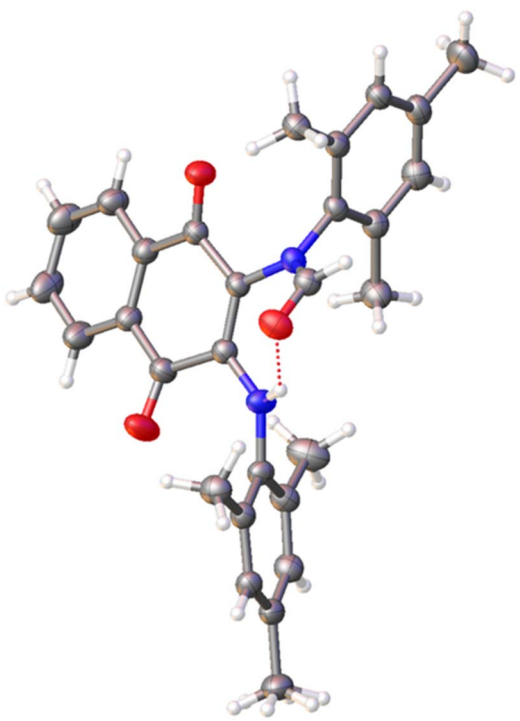

Fig. 7 Single crystal X-ray structure of **1′** with thermal ellipsoids drawn at the 50% probability level.

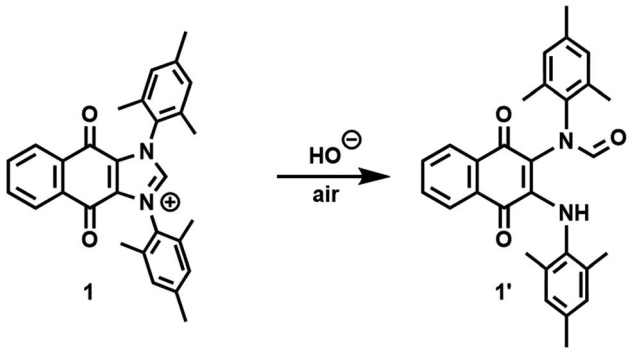

Fig. 8 Degradation of **1** in the presence of base to form compound **1′**.

solution as well (approximately 1.4 mM in MeCN at room temperature under 0.82 atm air).[25,26]

Monitoring the degradation pathway of **1** over time reveals much slower degradation when potential is not applied. ^{1}H NMR studies reveal that the slow accumulation of atmospheric water in dry CD_3CN solutions of **1** is sufficient to cause observable degradation, but that this process proceeds over months rather than hours. Electrogeneration of base, and/or consumption of HCl byproduct, is a necessary condition for the rapid and substantial conversion of **1** to **1′** upon air exposure. Therefore, although MeCN solutions of **1** are relatively stable in the absence of applied potential, **1** is unlikely to serve as an adequate direct air capture sorbent due to the simultaneous presence of atmospheric water and cathodic potentials during operation in low CO_2 concentration electrochemical conditions.

Analysis of sorbents **1–3** revealed that quinone-annulated imidazolium salts can achieve CO_2 binding strengths within the target range while also serving as dual-function sorbent-electrolytes as desired. Comparison across the three sorbents reveals that imidazolium functionalities have a substantial impact on the resulting reduction potential and nucleophilicity of the sorbent, and that an optimal sorbent requires only one positively charged imidazolium tag (**1** and **2**), whereas bisimidazolium structures are likely to have too great a positive shift in reduction potential to serve as adequate CO_2 binders (**3**). Additionally, comparison of **1** and **2** reveals that choice of *N*-alkyl or -aryl chains has relatively minimal impact on reduction potential and CO_2 binding strength. This observation may be leveraged to modulate properties such as solubility and solid packing without directly having a substantial impact on CO_2 binding strength.

Degradation of **1** to **1′** was confirmed in the presence of water (Fig. 8). It can be concluded that development of sorbents for solutions or ionic liquids with higher CO_2 capacity would require either higher solubility or more careful selection of substituents and counterions to achieve an ionic liquid. To achieve higher oxygen stability, on the other hand, structural modifications would need to be made to inhibit the observed degradation pathway of imidazolium ring opening at the C2 position.

With this in mind, we additionally designed novel quinone-annulated imidazolium salts **4**, **5**, and **6** as presented in Fig. 3. We hypothesized that butyl substitution at the C2 position would simultaneously achieve protection of the imidazolium ring from the reactivity shown in Fig. 11 while increasing organic solubility of the cation and disrupting solid packing. Results for ΔG_{bind} and the best-fit CO_2 binding stoichiometry for sorbents **4**, **5**, and **6** are reported in Table 1. DFT calculations corroborate both energetics and stoichiometry of binding of CO_2, thus supporting the experimental findings within experimental and DFT error. Additional details can be found in ESI Sections S10 and S11.† As hypothesized earlier, the CO_2 binding reactivity is preserved, which is further supported by a highly density of electrons localized on the reactive reduced oxygen atom shown in Fig. S11.1, S11.5, S11.9, and S11.13.†

Fig. 9 and S6.6† illustrate that the common cation shared for **5** and **6** appears to exhibit a more pronounced reoxidation feature than other quinones examined herein. Additionally, this feature lies substantially more positive in potential than those of other similar salts with comparable or even weaker binding. Despite the trend identified in previous work that weaker quinones tend to have milder release potentials, **5** and **6** exhibit $\Delta E_{release-capture}$ values over 600 mV compared to the 260 mV of their slightly stronger-binding analogue **4**.

Despite these differences, the peak shows a clear trend of growing in current under increasing CO_2 concentrations. Additionally, CVs of **6** taken with successively more negative switching potentials reveal that the oxidation peak at −0.7 V *vs.* Fc/Fc^+ grows in peak current with more time spent at potentials negative of the second reduction feature (Fig. S6.7†). For each extra −100 mV in switching potential, the system experiences an additional 2 seconds at potentials negative of $E_{capture}$, and the oxidation peak grows by a similar interval. This is consistent with an oxidation preceded by a chemical step; with additional time for the chemical step to occur, more of the species is present when the oxidation potential is reached, and more current is therefore observed.

The deviation in behavior of this oxidation feature as compared to other quinone carbon capture sorbents (and of sorbents **1**, **2**, and **4**) could potentially be explained by invoking the difference between concerted and stepwise dissociations (release of CO_2). In studies of stepwise *vs.* concerted dissociative electron transfer, Savéant reported that processes involving concerted mechanisms exhibit broader CV peaks (greater difference between $E_p - E_{p/2}$, and thereby, a transfer coefficient α deviating more widely from 0.5) and often, more positive potentials for reduction.[27] In a stepwise process, the electrode must directly place an electron into the lowest unoccupied molecular orbital (LUMO) of an analyte (or, in the case of sorbent reoxidation, remove an electron from the highest occupied molecular orbital HOMO). Then, a subsequent chemical step occurs in which a substituent is cleaved. However, in a concerted process, the observed reduction potentials are often milder than would be required based on the HOMO or LUMO alone. By this explanation, sorbents such as **4** could undergo concerted oxidation and release of CO_2; reoxidation features in the presence of CO_2 are broad and occur

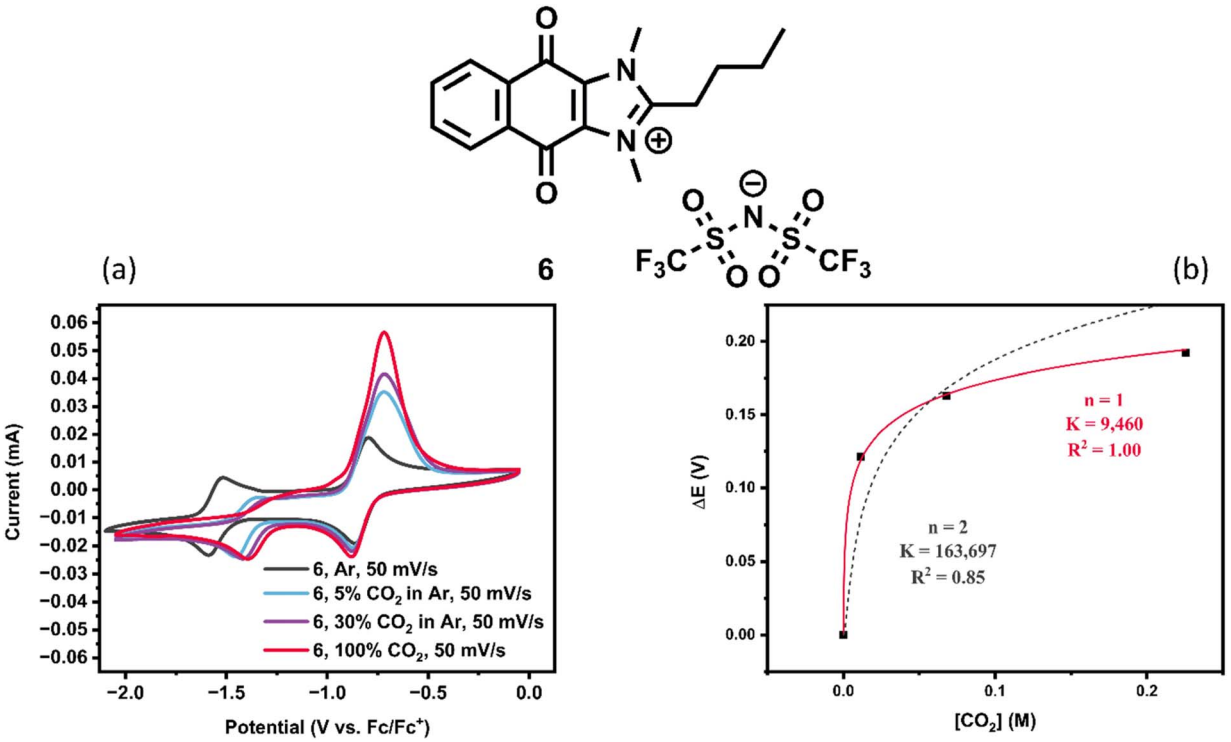

Fig. 9 (a) 1 mM CVs of **6** under varying concentrations of CO_2 (black under argon, cyan under 5% CO_2, purple 30% CO_2, red 100% CO_2) collected with a scan rate of 50 mV s^{-1} in 0.1 M NBu_4PF_6 in MeCN – WE glassy carbon, Pt wire counter electrode, reference externally *vs.* Fc/Fc^+. (b) Plot of ΔE *vs.* $[CO_2]$ fit to $\Delta E = \frac{RT}{F}\ln(K[CO_2]^n + 1)$ to find the equilibrium constant K and stoichiometry n of CO_2 molecules binding to sorbent.

close in potential to the reductions required for capture. On the other hand, **5** and **6** are hypothesized to undergo stepwise oxidation followed by dissociation of CO_2. This is consistent with both the sharper peak shape (*i.e.* more symmetrical barrier to electron transfer) and the more forcing potential required for oxidation. Confirmation of this hypothesis serves as a potential topic for future work.

In addition to the favorable binding and release of CO_2, comparable solubility studies to compounds **1**, **2**, and **3** were conducted with compounds **4**, **5**, and **6**. Compound **5** demonstrated poor solubility in MeCN and **4** was found to have similar solubilities to compounds **1**, **2**, and **3**, though compound **6** displayed a staggering 2.97 M solubility in MeCN (Table S5.1†). Compound **6** was selected for further study due to its high solubility in MeCN and stability over time (Fig. S8.6†). Compounds **1**–**6** when exposed to air in CV all show a shift in reduction potentials to more negative values and varied extents of lack of reversibility for the reduction waves (Fig. S6.1, S6.10–S6.13†). Unlike **1**–**5**, CVs taken of **6** at lower concentrations with supporting electrolyte in the presence of air displayed some of the original quinone waves unshifted (Fig. S6.13†), thus suggesting that some of the quinone is able to survive in aerobic conditions on the timescale of the CV measurement. Concentrated CVs were taken of **6** without supporting electrolyte to meet the high CO_2 capacity standards and O_2 stability requirements as outlined above. Similar results to compound **1** were obtained, indicating that compound **6** had the capacity to operate as its own supporting electrolyte with an ionic conductivity of 0.00741 S cm^{-1} for a 0.1 M solution (ESI Section S7†).

Fig. 10 shows CVs could be collected in the absence of supporting electrolyte, confirming the ability of salt **6** to serve as electrolyte. Large peak-to-peak separations ($E_{pc} - E_{pa}$) well above the theoretical 57 mV spacing are observed for both sorbents **1** (Fig. 6) and **6** under these conditions. This is especially noticeable for fast scan rates, as shown in Fig. 10. We attribute the disparity between the relative size of the two reduction waves to a disproportionation mechanism that is in effect when these quinones are probed at high concentrations.

Solutions in which **6** is the electrolyte (0.10 M, such as that used for the CVs) were analyzed by electrochemical impedance spectroscopy (EIS) to exhibit slightly higher ionic conductivity values compared to a standard 0.1 M NBu_4PF_6 electrolyte solution (0.00741 S cm^{-1} for **6** and 0.0068 S cm^{-1} for NBu_4PF_6, in a cylindrical cell of 1 cm^2 cross-sectional area with 1 cm electrode spacing). This high conductivity can also be seen at higher concentrations of sorbent **6**, where an ionic conductivity of 0.0196 S cm^{-1} at 0.8 M is observed which is lower than the 0.00741 S cm^{-1} of its 0.1 M counterpart (ESI Section S7†).

For **6**, the use of fast scan rates also allows for an additional observation. At relatively slow scan rates (50–100 mV s^{-1}), only a single reversible wave is observed. However, at fast scan rates (200–500 mV s^{-1}), a second reversible wave appears. This suggests that at slower scan rates, when chemical steps are allowed sufficient time to occur, reduction of the singly reduced

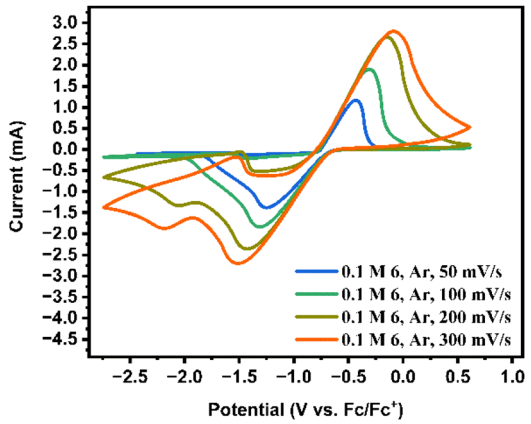

Fig. 10 Supporting electrolyte-free CVs of 0.1 M **6** in MeCN collected at scan rates of 50 mV s^{-1} (blue), 100 mV s^{-1} (green), 200 mV s^{-1} (brown), 300 mV s^{-1} (orange) – WE glassy carbon, Pt wire counter electrode, reference externally *vs.* Fc/Fc^{+}.

radical of **6** to the doubly reduced anion is not observed. This could indicate that disproportionation occurs under these conditions, as presented in Fig. 11. Under conditions with high loadings of **6** in solution, where collisions between reduced forms of **6** have increased likelihood, it may be possible to access the fully activated sorbent while only applying potential sufficient for the first reduction. This has important implications for the ability of **6** to operate in the presence of oxygen, as the first reduction potential of **6** (as measured in anhydrous MeCN with 0.1 M NBu_4PF_6) lies almost 400 mV positive of the oxygen reduction potential.

Sorbent **4** exhibits similar behavior, with only one reduction wave observed in CVs conducted at 0.1 M concentration. However, a full scan rate analysis was not possible, as current responses of **4** decreased with each successive CV scan, and color changes were rapidly observed in the solution.

Finally, the intended goal of structural modification of sorbents **1–3** by C2 alkylation was to impart increased stability to sorbents **4–6.** Most notably, **4** degrades rapidly in solution and under concentrated electrochemical testing conditions through a mechanism that involves apparent loss of a butyl group (ESI Section S8† for NMR stability studies). **5** and **6** are relatively more stable in the solution phase as evidenced by ^1H NMR monitoring, but **5** nonetheless degrades over the course of months in solution (ESI Section S8†), limiting the practicality of its use for electrochemical applications. ^1H NMR experiments of **5** revealed likely development of radical species simply from exposure to ambient conditions. However, as hypothesized for the exchange of the iodide counterion for the more stable bis-triflimide TFSI, sorbent **6** appears to exhibit improved solution-phase stability with no radical formation or degradation as observed by ^1H NMR up to one month.

In comparison to some sorbents in literature, compound **6** shows elevated ionic conductivity. We now show sorbent **6** to have higher ionic conductivity (Table 2) than previously reported cationic imidazolium functionalized quinones such as BAQMIM TFSI from Ueno and co-workers.[28] This discrepancy may arise from the imidazolium annulation of sorbent **6** *versus* the imidazolium functionalization of BAQMIM TFSI. Comparison between the two is difficult because of varying solvents used in these studies, with DMSO likely being the choice solvent due to limited solubility in other conditions. Other quinones with large solubilities in organic solvents including LQ (Table 2) from Hatton and co-workers achieved a lower solubility than compound **6** as well as a lower ionic conductivity.[29] In concentrated solutions of **6**, the $E_{release-capture}$ metric is larger than BAQMIM TFSI and lower than LQ, indicating that work can still be done to improve the voltage efficiency of capture and release. Sorbent **6** aligns itself with literature standards and provides promise for use as a dual electrolyte and CO_2 sorbent.

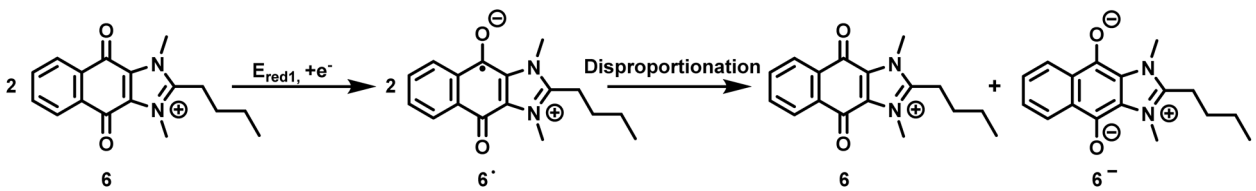

Fig. 11 Proposed disproportionation mechanism for compound **6** showing that reduction only at the first reduction potential, E_{red1}, may allow access to the doubly reduced sorbent state.

Table 2 Comparison of sorbents

Quinone	$E_{release-capture}$ (V)	Electrolyte	Ionic conductivity (S cm^{-1})	Solubility
BAQMIM TFSI[a]	0.15	1 M [P13][TFSI] in DMSO	0.0122 in DMSO	3.98 M in DMSO
1	0.32	None	0.00253 in MeCN	0.12 M in MeCN
4	0.26	None	0.00469 in MeCN	0.16 M in MeCN
5	0.61	None	0.00171 in MeCN	0.02 M in MeCN
6	0.67	None	0.0196 in MeCN	2.87 M in MeCN
LQ[b]	1	NaTFSI in DEGME[c]	0.00249 in Diglyme	1.484 M in DEGME[c]

[a] 1-Butyl-3-((2′-anthraquinoyl)methyl)imidazolium bis(trifluoromethanesulfonyl)amide.[28] [b] 2,3-Bis(2-(2-methoxyethoxy)ethoxy)naphthalene-1,4-dione.[29] [c] 2-(2-Methoxyethoxy)ethanol.

Conclusions

Through the synthesis and characterization of quinone-annulated imidazolium salts, we have now found molecular sorbents for CO_2 capture that show promising activity as both sorbent and electrolyte in these applications. Specifically, through iterative design and stability studies coupled with cyclic voltammetry, conductivity measurements, and corroboration by density functional theory (DFT), we now find that C2 alkyl substitution of the imidazolium moiety of these salts, along with judicious choice of counterion, is critical for stability of the sorbent. Across these several synthetic iterations, we identified a C2-butylated quinone-annulated imidazolium bis-triflimide **6** salt that possesses promising CO_2 binding strengths for capture of CO_2 from dilute sources, relatively small potential difference (ΔE) between the voltage needed for capture and release, a relatively high solubility (2.87 M) in anhydrous acetonitrile, and sufficient solution conductivity to operate as its own electrolyte. This work sets the stage for the design of ionic molecular materials that can act as both reactive sorbents and electrolytes that could ultimately allow for organic redox battery-like operation of redox-swing systems.

Though the sorbents presented in this work are organic ionic species dissolved in solution, we additionally hope to improve the oxygen stability of imidazolium annulated quinone sorbents through structural modification and their conversion into an ionic liquid. We remain forward looking to future developments in this area and anticipate future applications of iterative structure property functions studies towards the design of molecular materials for these applications.

Data availability

Data described in this manuscript is available in the ESI files† (inclusive of .cif, checkCIF, .xyz files). The crystal structure has been deposited to the Cambridge Structural Database with deposition number 2417570.

Author contributions

The manuscript was written through contributions of all authors/all authors have given approval to the final version of the manuscript.

Conflicts of interest

There are no conflicts to declare.

Abbreviations

CCUS	Carbon capture, utilization, and storage
CV	Cyclic voltammetry
DAC	Direct air capture
RTIL	Room-temperature ionic liquid

Acknowledgements

This material is based upon work supported by the National Science Foundation Graduate Research Fellowship under Grant No. DGE 2040434. AML thanks the Graduate Assistance in Areas of National Need (GAANN) Fellowship awarded to CU-Boulder (Award No. P200A210114). We also thank the University of Colorado Boulder for generous startup support. We would like to thank Dr Matthias Zeller and the American Crystallographic Association Summer Course in Chemical Crystallography for assistance with solving and refining the structure of **1′**. HAP thanks the National Science Foundation Graduate Research Fellowship Program.

References

1 S. Voskian and T. A. Hatton, Faradaic electro-swing reactive adsorption for CO_2 capture, *Energy Environ. Sci.*, 2019, **12**(12), 3530–3547.
2 X. Li, X. Zhao, L. Zhang, A. Mathur, Y. Xu, Z. Fang, L. Gu, Y. Liu and Y. Liu, Redox-tunable isoindigos for electrochemically mediated carbon capture, *Nat. Commun.*, 2024, **15**(1), 1175.
3 J. M. Barlow and J. Y. Yang, Oxygen-Stable Electrochemical CO_2 Capture and Concentration with Quinones Using Alcohol Additives, *J. Am. Chem. Soc.*, 2022, **144**(31), 14161–14169.
4 J. Wilcox, An electro-swing approach, *Nat. Energy*, 2020, **5**(2), 121–122.
5 M. Massen-Hane, K. M. Diederichsen and T. A. Hatton, Engineering redox-active electrochemically mediated carbon dioxide capture systems, *Nat. Chem. Eng.*, 2024, **1**(1), 35–44.
6 H. Seo and T. A. Hatton, Electrochemical direct air capture of CO_2 using neutral red as reversible redox-active material, *Nat. Commun.*, 2023, **14**(1), 313.
7 P. Scovazzo, J. Poshusta, D. DuBois, C. Koval and R. Noble, Electrochemical separation and concentration of <1% carbon dioxide from nitrogen, *J. Electrochem. Soc.*, 2003, **150**(5), D91.
8 K. Lin, R. Gómez-Bombarelli, E. S. Beh, L. Tong, Q. Chen, A. Valle, A. Aspuru-Guzik, M. J. Aziz and R. G. Gordon, A redox-flow battery with an alloxazine-based organic electrolyte, *Nat. Energy*, 2016, **1**(9), 16102.
9 B. Yang, L. Hoober-Burkhardt, S. Krishnamoorthy, A. Murali, G. K. S. Prakash and S. R. Narayanan, High-Performance Aqueous Organic Flow Battery with Quinone-Based Redox Couples at Both Electrodes, *J. Electrochem. Soc.*, 2016, **163**(7), A1442–A1449.
10 K. Lin, Q. Chen, M. R. Gerhardt, L. Tong, S. B. Kim, L. Eisenach, A. W. Valle, D. Hardee, R. G. Gordon, M. J. Aziz and M. P. Marshak, Alkaline quinone flow battery, *Science*, 2015, **349**(6255), 1529–1532.
11 M. Abdinejad, M. Massen-Hane, H. Seo and T. A. Hatton, Oxygen-Stable Electrochemical CO_2 Capture using Redox-Active Heterocyclic Benzodithiophene Quinone, *Angew. Chem., Int. Ed.*, 2024, e202412229.

12 H. A. Petersen and O. R. Luca, Application-specific thermodynamic favorability zones for direct air capture of carbon dioxide, *Phys. Chem. Chem. Phys.*, 2021, **23**(22), 12533–12536.
13 A. W. Alherz, H. A. Petersen, N. R. Singstock, S. N. Sur, C. B. Musgrave and O. R. Luca, Predictive energetic tuning of quinoid O-nucleophiles for the electrochemical capture of carbon dioxide, *Energy Adv.*, 2022, **1**(11), 900–907.
14 H. S. Yu, X. He, S. L. Li and D. G. Truhlar, MN15: A Kohn–Sham global-hybrid exchange–correlation density functional with broad accuracy for multi-reference and single-reference systems and noncovalent interactions, *Chem. Sci.*, 2016, **7**(8), 5032–5051.
15 M. D. Sanderson, J. W. Kamplain and C. W. Bielawski, Quinone-Annulated N-Heterocyclic Carbene–Transition-Metal Complexes: Observation of π-Backbonding Using FT-IR Spectroscopy and Cyclic Voltammetry, *J. Am. Chem. Soc.*, 2006, **128**(51), 16514–16515.
16 O. R. Luca, D. L. Huang, M. K. Takase and R. H. Crabtree, Redox-active cyclopentadienyl Ni complexes with quinoid N-heterocyclic carbene ligands for the electrocatalytic hydrogen release from chemical fuels, *New J. Chem.*, 2013, **37**(11), 3402.
17 A. G. Tennyson, V. M. Lynch and C. W. Bielawski, Arrested Catalysis: Controlling Kumada Coupling Activity *via* a Redox-Active N-Heterocyclic Carbene, *J. Am. Chem. Soc.*, 2010, **132**(27), 9420–9429.
18 J. S. Park, E. Karnas, K. Ohkubo, P. Chen, K. M. Kadish, S. Fukuzumi, C. W. Bielawski, T. W. Hudnall, V. M. Lynch and J. L. Sessler, Ion-Mediated Electron Transfer in a Supramolecular Donor-Acceptor Ensemble, *Science*, 2010, **329**(5997), 1324–1327.
19 K. M. Kuhn and R. H. Grubbs, A Facile Preparation of Imidazolinium Chlorides, *Org. Lett.*, 2008, **10**(10), 2075–2077.
20 J. Yuan, Z. Liu, Y. Dong, F. Gao, X. Xia, P. Wang, Y. Luo, Z. Zhang, D. Yan and W. Zhang, Pioneering 4,11-Dioxo-4,11-dihydro-1H-anthra[2,3-d]imidazole-3-ium Compounds as Promising Survivin Inhibitors by Targeting ILF3/NF110 for Cancer Therapy, *J. Med. Chem.*, 2023, **66**(24), 16843–16868.
21 M. T. Huynh, C. W. Anson, A. C. Cavell, S. S. Stahl and S. Hammes-Schiffer, Quinone 1 e- and 2 e-/ 2 H+ Reduction Potentials: Identification and Analysis of Deviations from Systematic Scaling Relationships, *J. Am. Chem. Soc.*, 2016, **138**(49), 15903–15910.
22 U. Salma and N. Shalahin, A mini-review on alkaline stability of imidazolium cations and imidazolium-based anion exchange membranes, *Results Mater.*, 2023, **17**, 100366.
23 D. Döpp, M. A.-M. Gomaa, G. Henkel and A. M. N. El-Din, Reaction of N1, N2-diarylamidines with chloranil and 2,3-dichloro-1,4-naphthoquinone, *J. Heterocycl. Chem.*, 1995, **32**(2), 603–610.
24 H.-J. Lee, J. Choi, J. Y. Han, H.-J. Kim, Y.-E. Sung, H. Kim, D. Henkensmeier, E. Ae Cho, J. H. Jang and S. J. Yoo, Synthesis and characterization of poly(benzimidazolium) membranes for anion exchange membrane fuel cells, *Polym. Bull.*, 2013, **70**(9), 2619–2631.
25 D. T. Sawyer, G. Chiericato, C. T. Angelis, E. J. Nanni and T. Tsuchiya, Effects of media and electrode materials on the electrochemical reduction of dioxygen, *Anal. Chem.*, 1982, **54**(11), 1720–1724.
26 P. S. Singh, *The Electrochemical Reduction of Superoxide in Acetonitrile: A Concerted Proton-Coupled Electron Transfer (PCET) Reaction*, University of Arizona, Tucson, AZ, 2005.
27 J.-M. Savéant, Electron transfer, bond breaking and bond formation, in *Advances in Physical Organic Chemistry*, Academic Press, 2000, vol. 35, pp 117–192.
28 H. Iida, S. Kondou, S. Tsuzuki, M. Tashiro, N. Shida, K. Motokura, K. Dokko, M. Watanabe and K. Ueno, Imidazolium-Functionalized Anthraquinone for High-Capacity Electrochemical CO_2 Capture, *J. Phys. Chem. C*, 2023, **127**(21), 10077–10086.
29 K. M. Diederichsen, Y. Liu, N. Ozbek, H. Seo and T. A. Hatton, Toward solvent-free continuous-flow electrochemically mediated carbon capture with high-concentration liquid quinone chemistry, *Joule*, 2022, **6**(1), 221–239.